Structural studies of *N*-(2′-substituted phenyl)-9,10-dihydro-9,10-ethanoanthracene-11,12-dicarboximides by X-ray diffraction and NMR spectroscopy—proofs for CH/π interactions in liquid and solid phases†

Gisbert Grossmann,*‡[a] Marek J. Potrzebowski,*[a] Sebastian Olejniczak,[a] Natasza E. Ziółkowska,[b] Grzegorz D. Bujacz,[b] Wlodzimierz Ciesielski,[a] Wiktor Prezdo,[c] Valerii Nazarov[d] and Vladislav Golovko[d]

[a] *Center of Molecular and Macromolecular Studies, Polish Academy of Sciences, Sienkiewicza 112, 90-363, Łódź, Poland. E-mail: marekpot@bilbo.cbmm.lodz.pl; Fax: +48 42 684 7126; Tel: +48 42 684 4014*

[b] *Institute of Technical Biochemistry, Technical University of Lodz, Stefanowskiego 4/10, 90-924, Łódź, Poland. E-mail: gdbujacz@ck-sg.p.lodz.pl; Fax: +48 42 631 3402; Tel: +48 42 631 3431*

[c] *Institute of Chemistry, Swietokrzyska Academy, Checinska 5, 25-020, Kielce, Poland. E-mail: wiktor.prezdo@pu.kielce.pl*

[d] *Department of Organic Chemistry, Kharkov Polytechnic Institute, Frunze 21, 61-002 Kharkov, Ukraine*

Received (in Toulouse, France) 20th January 2003, Accepted 27th February 2003
First published as an Advance Article on the web 9th June 2003

N-(2′-*R*-Phenyl)-9,10-dihydro-9,10-ethanoanthracene-11,12-dicarboximides with R = Me (**1**), OMe (**2**), OEt (**3**) and H (**4**) were investigated. The crystal and molecular structures of **1**–**3**, determined by single crystal methods, show different conformations of the *N*-(2′-*R*-phenyl) group. *Anti* conformations and weak intermolecular CH/π contacts were found in **2** and **3**, while *anti* and *syn* conformations coexist in **1** with CH/π contacts being absent. Solid-state ^{13}C CP/MAS spectra confirm the X-ray molecular structural data. Two crystallographically independent molecules in the unit cell of **2** correspond to two isotropic chemical shifts for C atoms in the CP/MAS spectrum. The different molecular dynamics of both molecules in the crystal lattice of **2** indicated by the thermal factors and intermolecular CH/π contacts were clearly visible in different cross-polarisation profiles. The NMR data of **4** suggest that the phenyl ring bonded to the nitrogen is nearly coplanar to the ethanocarboximide ring. Full assignment of liquid state ^{1}H and ^{13}C NMR spectra of **1**–**4** was possible by application of high field NMR spectroscopy. Some incorrect assignments of ^{13}C chemical shifts in the literature were revised. The different ratios of [*syn*]:[*anti*] in solutions of chloroform and DMSO are explained in terms of different intermolecular CH/π interactions.

Introduction

Weak intra- and intermolecular interactions play an important role in crystal engineering, supramolecular chemistry, molecular recognition and self-organisation of molecules.[1] Different types of contacts, including C–H···O, C–H···N, OH/π, NH/π, CH/π interactions, have been reported recently.[2] Knowledge about the nature of weak interactions combined with the known geometry of supramolecular synthons makes it now possible to construct supramolecular motifs in the solid phase.[3]

Much attention has been paid to CH/π forces, which can control both molecular packing and intramolecular dynamics.[4] For instance, the height of a rotational barrier and the ratio of different conformation states of a molecule depend not only on the spatial dispositions and electrostatic interactions, but also on weak interactions as hydrogen bonds and CH/π contacts. The influence of intra- and intermolecular CH/π interactions on the ratio of the *syn* and *anti* conformations of *N*-(2′-methyl-4′-nitrophenyl)-9,10-dihydro-9,10-ethanoanthracene-11,12-dicarboximide in solutions and crystals was investigated by Kishikawa *et al.*[5] Verma and Singh[6a] initiated a study of the conformations around the aryl N–C bond for this class of compounds. A number of papers dealing with this problem used mostly routine ^{1}H NMR spectroscopy[6b–d] and in one case ^{13}C NMR.[6e] Unfortunately, for some samples the line assignment was ambiguous because the magnetic field strengths of the used spectrometers were not sufficient to resolve all lines.

As a part of our continuing interest in understanding the role of weak contacts in molecular architectures and the correlation between liquid and solid phases by employing different spectroscopic techniques,[7] we report in this paper results of studies on *N*-(2′-substituted phenyl)-9,10-dihydro-9,10-ethanoanthracene-11,12-dicarboximides, **1**–**3** (see Scheme 1). Our

† Electronic supplementary information (ESI) available: figures of the conformations in compound **1** and the molecular packing and intermolecular CH/π interactions in compounds **2** and **3**. See http://www.rsc.org/suppdata/nj/b3/b300759f/

‡ New address: Neukircher Str. 13, D-01920 Haselbachtal, Germany. E-mail: Gisbert.Grossmann@t-online.de; Fax: +49 3578 306 776; Tel: +49 3578 306 774.

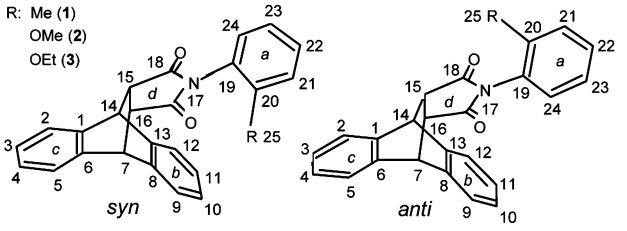

Scheme 1 (see ref. 8).

project was carried out in several stages. First, the molecular and crystal structures were determined. Secondly, a full assignment of the signals of the ^{1}H and ^{13}C spectra to the atom positions in solution was carried out using high-resolution 1D and 2D spectra recorded on a 500 MHz spectrometer in [D_6]DMSO and in $CDCl_3$. This allowed us to monitor the differences of the ^{1}H and ^{13}C chemical shifts of all atoms between the *syn* and *anti* conformations and to study the solvent-solute interactions. Thirdly, we used the possibilities of ^{13}C high-resolution solid-state NMR spectroscopy to investigate the molecular structure, packing effects and molecular dynamics. In the second and third phases, we have included investigations of the "parent" compound *N*-phenyl-9,10-dihydro-9,10-ethanoanthracene-11,12-dicarboximide, **4**.

Experimental

Preparation

The powdered Diels–Alder adduct of anthracene with maleic anhydride (0.01 mol) was mixed with one of the aromatic amines (0.01 mol). The reaction mixture was heated 3 h at 140–150 °C.[6a] The reaction product was repeatedly recrystallised from toluene. The target products were obtained with a yield of about 70%. The ^{1}H and ^{13}C NMR data are given in Table 3 in the Results section.

N-(2′-Methylphenyl)-9,10-dihydro-9,10-ethanoanthracene-11,12-dicarboximide, **1**. M.p. 247 °C (lit.[9] 248 °C).

N-(2′-Methoxyphenyl)-9,10-dihydro-9,10-ethanoanthracene-11,12-dicarboximide, **2**. M.p. 265 °C (lit.[6a] 266–268 °C).

N-(2′-Ethoxyphenyl)-9,10-dihydro-9,10-ethanoanthracene-11,12-dicarboximide, **3**. M.p. 193 °C.

N-Phenyl-9,10-dihydro-9,10-ethanoanthracene-11,12-dicarboximide, **4**. M.p. 228–230 °C (lit.[6a] 230–231 °C).

X-Ray crystallographic studies

Single crystals of compounds **1**–**3** were obtained by recrystallisation from toluene. Crystal and molecular structure was determined using data collected at room temperature on a CAD4 diffractometer with graphite monochromated $Cu_{K\alpha}$ radiation ($\lambda = 1.54184$ Å). Maximum 2θ was 150°, scan mode $\omega/2\theta$, scan width $1.25° + 0.14{\cdot}\tan\theta$ (**1**) and $0.95 + 0.14{\cdot}\tan\theta$ (**2** and **3**). The lattice constants were refined by least-squares fits of 25 reflections in the θ ranges of 22.00–27.35° (**1**), 20.94–27.22° (**2**) and 20.93–27.20° (**3**). The decline in intensities of three control reflections was −3.4% for **1**, −1% for **2** and 13.6% for **3** for exposure times of 177.5, 107.8 and 107.9 h, respectively. Intensity corrections (DECAY program)[10] and empirical absorption corrections (ψ-scan method; EAC program)[10,11] were applied for all compounds. All observed reflections with $I > 0\sigma(I)$ were used to solve the structure by direct methods and to refine it by full-matrix least-squares using F.[12,13] Hydrogen atoms were found on difference Fourier maps and refined isotropically, except for H atoms attached to the disordered methylphenyl substituent in **1**. These atoms were placed geometrically at idealised positions and set as riding with fixed thermal parameters equal to 1.3 times the equivalent isotropic thermal parameter of the parent atom. Anisotropic thermal parameters were refined for all nonhydrogen atoms. Data correction was carried out with the Enraf–Nonius SDP crystallographic computing package;[10] structure solution with SHELXS;[12] and structure refinement with SHELXL.[13] Selected crystal data and experimental details are shown in Table 1.

Table 1 Selected crystal data and some details of the refinement calculations for **1**–**3**

Compound	**1**	**2**	**3**
Molecular formula	$C_{25}H_{19}NO_2$	$C_{25}H_{19}NO_3$	$C_{26}H_{21}NO_3$
Formula mass	365.41	381.41	395.44
Crystal system	Trigonal	Triclinic	Monoclinic
T/K	293(2)	293(2)	293(2)
μ/mm^{-1}	0.634	0.700	0.690
a/Å	18.949(2)	10.489(3)	10.900(2)
b/Å	18.949(2)	10.626(2)	12.637(3)
cÅ	18.949(2)	17.737(3)	15.214(4)
α/°	117.25(2)	79.166(14)	90.0
β/°	117.25(2)	79.92(2)	108.16(2)
γ/°	117.25(2)	89.27(2)	90.0
Space group	$R\bar{3}$ (no.148)	$P\bar{1}$ (no.2)	$P2_1/c$ (no.14)
Z	6	4	4
D/g cm^{-3}	1.264	1.325	1.319
Unique reflect.	3956	7869	4100
Obs. reflect. [$I > 0\sigma(I)$]	3838	7536	3981
Obs. reflect. [$I > 2\sigma(I)$]	3482	6884	3698
R_{int}	0.0502	0.0197	0.0380
R_{obs}	0.0436	0.0463	0.0440
wR_{obs}	0.1124	0.1338	0.1207
n	0.2737	0.4231	0.3164
m	0.0549	0.0740	0.0731

[a] Weighting scheme: $w = [\sigma^2(F_o^2) + (mP)^2 + nP]^{-1}$, where $P = (F_o^2 + 2F_c^2)/3$.

CCCD reference numbers 196632–196634. See http://www.rsc.org/suppdata/nj/b3/b300759f/ for crystallographic files in CIF or other electronic format.

Solution and solid-state NMR

Solution-state NMR spectra were recorded on a Bruker Avance DRX 500 spectrometer operating at 500.13 MHz for ^{1}H and 125.258 MHz for ^{13}C. The chemical shift of the DMSO or chloroform signal was used as a reference ($\delta = 2.49$ or 7.26 ppm for ^{1}H and $\delta = 39.5$ or 77.0 ppm for ^{13}C, respectively). The spectrometer was equipped with a pulsed field gradient unit (50 G·cm^{-1}). Twenty-five milligrams of samples were dissolved in 0.5 ml of the solvent for the ^{13}C and 2D spectra while the ^{1}H spectra were recorded at lower concentration (5 mg in 0.5 ml).

The solid-state ^{13}C CP/MAS NMR experiments were performed on a Bruker Avance DSX 300 spectrometer at 75.47 MHz frequency, equipped with a MAS probehead using 4 mm ZrO_2 rotors. The conventional spectra were recorded with a proton 90 degree pulse length of 4.0 μs and a contact time of 1 ms. The repetition delay was 10 s and the spectral width was 25 kHz. The FIDs were accumulated with a time domain size of 2K data points. The RAMP shape pulse was used during the cross-polarisation[14] and TPPM with $\tau_p = 7.2$ μs and a phase angle of 20° during the acqusition.[15] The dipolar dephasing spectra were recorded with a dephasing time of 40 μs.[16–18] The cross-polarisation efficiency was measured using rectangular pulses for cross-polarisation with contact times between 10 μs and 12 ms and with a spinning rate of 4000 Hz. Data were processed using the WIN-NMR program.[19] A sample of glycine was used for setting the Hartmann–Hahn condition and as the shift reference: $\delta = 176.04$ ppm (C=O).

Results and discussion

X-Ray single crystal studies

The molecular structures of compounds **1**–**3** are shown in Fig. 1. The structures of the dihydroethanoanthracenedicarboximide skeleton are very similar, while the location of the *N*-phenyl substituent is different (see Table 2).

The molecules of **2** and **3** have the *ortho*-alkoxyphenyl group in the expected *anti* conformation but a more complex situation was found for compound **1**. The atoms of the methylphenyl group cannot be localised on single atomic positions. In the refinement of the structure, the peaks on the electron density difference Fourier map could be connected to three conformations. Three sets of atomic positions for this group led to a satisfactory solution: one set corresponds with a *syn* conformation and two sets give two different *anti*-conformations (see Scheme 2). There are two possibilities: either the *syn* and *anti* conformations are trapped in the crystallisation, or this is a rare case in which the conformation of such a bulky group may change in the solid state. As the low density (1.26 $g \cdot cm^{-1}$) indicates, the spatial packing is not very high. Therefore, a slow motion of a bulky molecular part is possible. The different conformations are probably statistically distributed.

The existence of an *anti* conformation of the 2′-methyl-4′-nitrophenyl group in the crystal of a compound similar to **1**,[5] was explained by those authors by intermolecular CH/π interactions. These interactions compensate the intramolecular CH/π interactions that are present in the *syn* conformation existing in solution.

In compound **1** intermolecular CH/π interactions do not play any role. The shortest $CH_3 \cdots C_{sp^2}$ distances to the rings *b* or *c* are greater then 4.0 Å. Such interactions are effective only if the distances are shorter than 3.7 Å (or $H \cdots C_{sp^2} < 3.1$ Å).[20] The molecules related by a threefold axis can never adopt the *anti*-1 conformation at the same time, because then the distances between two methyl groups are too small. The distances between C25′ and the symmetrically related ($-1+y$, $1+z$, *x* or *z*, $1+x$, $-1+y$) C25′ are 3.14 Å. For a graphical picture of some chosen arrangements see the Electronic supplementary information (ESI).

Molecule 1 of compound **2** does not show CH/π interactions while molecule 2 has six intermolecular contacts between H25B and ring *c* (2.78, 2.81, 2.90, 2.95, 3.02 and 3.04 Å for C3′, C4′, C2′, C5′, C1′ and C6′, respectively) and two contacts in each case with rings *b* and *c* (H25A: 2.98 and 3.05 Å for C1′ and C13′; H25C: 3.05 and 3.15 Å for C8′ and C6′). A graphical picture of the CH/π contacts is given in the ESI. Molecules 1 and 2 differ also by the dihedral angles between rings *a* and *b* (see Table 2). Additionally, the average thermal factor for molecule 1 is 20% higher than for molecule 2 (for the carbon of the methyl group the thermal factor of C25 is even 71% higher than of C25′).

Compound **3** has intermolecular CH/π interactions between H261 and ring *b* (2.97 and 3.10 Å for C12 and C13) and

Table 2 Selected bond lengths (Å), bond angles and dihedral angles[a] (°)

Compound	N–C(19)	C(17)–N–C(19)	C(18)–N–C(19)	Dihedral angle
1: *syn*	1.438(8)	129.1(4)	117.8(4)	79.00(14)
1: *anti*-1	1.533(11)	117.6(5)	129.2(5)	68.33(24)
1: *anti*-2	1.376(7)	118.6(5)	126.3(4)	79.90(18)
2: molecule 1	1.434(2)	122.5(1)	124.6(1)	88.99(7)
2: molecule 2	1.429(2)	123.3(1)	123.2(1)	83.02(7)
3	1.431(2)	123.8(1)	123.0(1)	87.11(3)

[a] Dihedral angle between rings *a* and *b* (see Scheme 1).

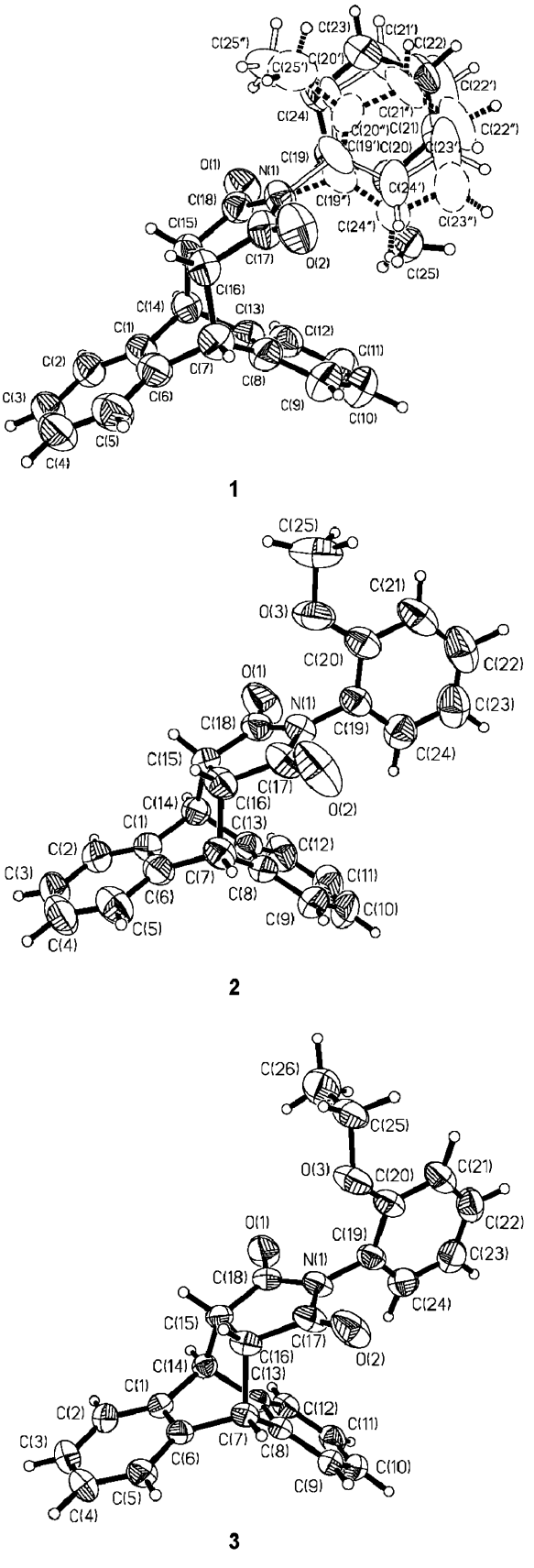

Fig. 1 ORTEP views of compounds **1**–**3**. For compound **1**, the *syn* conformation of the disordered phenyl ring is shown with a solid bond and normal ellipsoids. The two *anti* conformations are drawn with dashed bonds and ellipsoids and with unfilled bonds and ellipsoids. For compound **2**, only molecule 1 is shown.

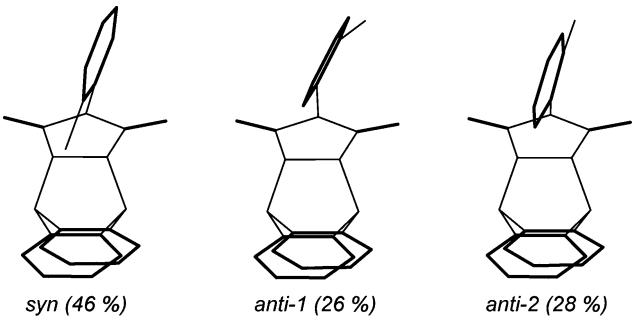

Scheme 2 The three conformations of the 2′-methylphenyl group in crystalline compound **1**.

between H252 and ring *b* (2.89, 2.93, 3.01 and 3.06 Å for C11, C12, C10 and C13, respectively). A graphical picture of the CH/π contacts can be seen in the ESI.

Solution NMR

The ^{1}H and ^{13}C chemical shifts of compounds **1**–**4** are summarised in Table 3. Because the spectra in [D_6]DMSO solution generally show some bigger differences between the chemical shifts of the *syn* and *anti* conformations, these are the data chosen for this table.

2D COSY and 2D TOCSY spectra were recorded to locate the overlapping signals and to assign all ^{1}H signals to the proton numbers.[21] Fig. 2 shows the aromatic part of the COSY spectrum of compound **2**. The overlapping signals of H22s, H22a and H10/11a can be precisely located, as well as the H21s and H23s signals. Cross peaks in the 2D NOESY spectra between protons H25s and H24a and the respective protons from the *b* ring, H10/11 and/or H9/12, confirmed the structure assignment. All protons have different chemical shifts for the two conformations. The biggest difference was obtained by ring current shielding from the *b* ring to H24a and moderate shielding effects are shown on H23a, H25s, H26s and H21s.

An unambiguous assignment of all ^{13}C lines to the atoms is based on the assigned proton signals and the 2D HMQC and HMBC spectra, which also allow to distinguish the overlapped lines.[22] All carbon atoms show different chemical shifts for the

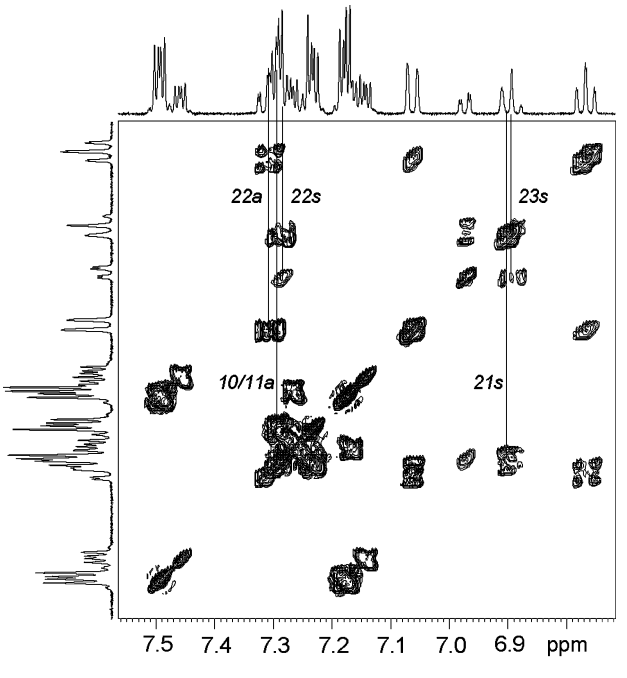

Fig. 2 COSY spectrum of the aromatic part of **2** (without the signal at 5.38 ppm).

Table 3 ^{1}H and ^{13}C chemical shifts (ppm) for compounds **1**–**4** recorded at 25 °C in [D_6]DMSO (referenced internally to the solvent signal using the values of 2.49 ppm for ^{1}H and 39.5 ppm for ^{13}C)

Position number	Atom	**1**		**2**		**3**		**4**
		syn	*anti*	*syn*	*anti*	*syn*	*anti*	
1/6	C	142.25	141.64	142.51	141.60	142.59	141.55	141.61
2/5	H	7.158	7.187	7.147	7.182	7.140	7.181	7.185
	C	126.28	126.40	126.20	126.39	126.12	126.33	126.34
3/4	H	7.475	7.504	7.462	7.497	7.456	7.494	7.501
	C	124.25	124.39	124.17	124.41	124.12	124.35	124.34
7/14	H	4.866	4.854	4.810	4.839	4.815	4.840	4.851
	C	44.40	44.86	44.44	44.95	44.32	44.93	44.84
8/13	C	139.85	139.41	139.50	139.43	139.56	139.33	139.28
9/12	H	7.142	7.243	7.122	7.237	7.140	7.229	7.205
	C	126.84	126.68	126.39	126.65	126.33	126.59	126.61
10/11	H	7.327	7.308	7.270	7.295	7.273	7.294	7.296
	C	125.13	124.90	124.92	124.92	124.77	124.85	124.77
15/16	H	3.418	3.483	3.359	3.498	3.358	3.494	3.399
	C	46.77	46.65	46.83	46.44	46.88	46.34	46.61
17/18	C	175.90	175.90	175.34	175.63	175.27	175.49	175.92
19	C	131.44	131.06	120.59	120.34	121.08	120.68	131.81
20	H	–	–	–	–	–	–	6.416
	C	135.52	135.60	154.62	154.77	153.27	153.83	126.52
21	H	7.118	7.235	6.900	7.067	6.933	7.057	7.315
	C	130.31	130.52	112.10	112.40	112.89	113.53	128.82
22	H	7.232	7.218	7.286	7.311	7.262	7.280	7.31
	C	128.97	129.07	130.24	130.65	130.05	130.46	128.44
23	H	7.19	7.016	6.898	6.770	6.868	6.758	7.315
	C	126.40	126.35	119.96	120.27	119.66	120.15	128.82
24	H	6.997	5.325	6.976	5.375	6.973	5.449	6.416
	C	128.11	127.11	129.04	128.28	129.20	128.15	126.52
25	H	0.921	1.978	3.328	3.664	3.768	3.966	–
	C	15.71	17.06	55.23	55.61	62.61	63.82	–
26	H	–	–	–	–	0.960	1.145	–
	C	–	–	–	–	13.77	14.30	–

syn and *anti* conformations. Fig. 3 demonstrates this using compound **2** as an example. Only the lines of 10/11s and 10/11a are not resolved. The unexpected high differences $\Delta = \delta_{syn} - \delta_{anti}$ for atoms C1/6 of the *c* ring (0.6, 0.9 and 1.0 ppm for **1**, **2** and **3**, respectively) show that the intramolecular CH/π interactions between protons H25s (and H26s) and the π system of ring *b* were transmitted to ring *c*.

It is understandable that the ^{1}H and ^{13}C chemical shifts of the *anti* conformation of the dihydroanthracene skeleton of **1**–**3** are very similar to those of the "parent" compound **4** while the *syn* values differ remarkably because the 2′ substituent is absent. The most significant diagnostic tool is H24. The experimental value $\delta_{H24} = 6.42$ ppm for **4** is distinctly higher than the mean values of both conformations in **1**–**3** (6.16–6.21 ppm). It may be concluded that the phenyl group in **4** rotates freely about the N–C bond or, if a small barrier exists, then the conformations have other angles between rings *a* and *b* than in compounds **1**–**3**.

It is well known that the ratio of conformers, determined in different solvents, differ from each other. The [*syn*]/[*anti*] ratio of the conformations, for the investigated class of compounds, is always lower in chloroform than in DMSO (see Table 4). This can be explained by formation of a CD/π complex between a solvent molecule and the upside face of ring *b*,

Table 4 [*syn*]/[*anti*] ratio in $CDCl_3$ and [D_6]DMSO[a]

Compound	Solvent	
	$CDCl_3$	[D_6]DMSO
1	0.78	1.30
2	0.25	0.40
3	0.08	0.23

[a] The ratios are mean values from 4–7 signals.

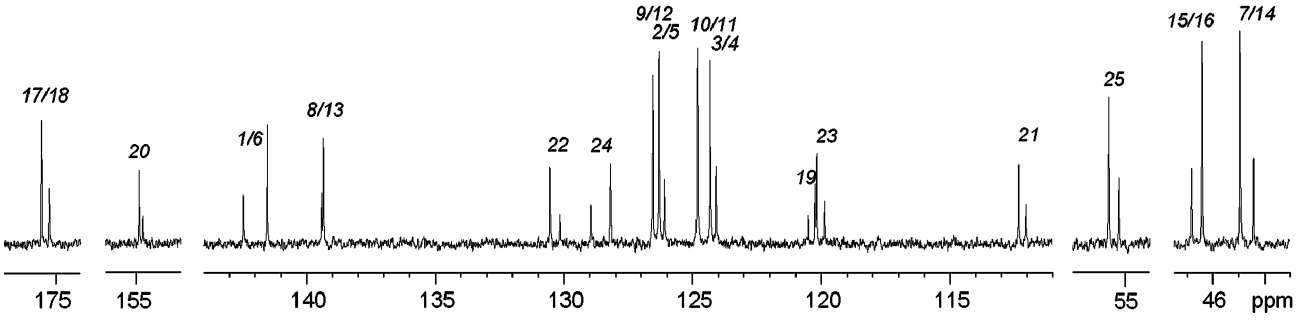

Fig. 3 Selected regions of the ^{13}C spectrum of a solution of **2** in [D_6]DMSO. The higher peaks result from *anti* conformations, the lower from *syn*.

disturbing the stabilisation of the *syn* conformation. Such a complex with chloroform is probably more stable than one with DMSO. The increasing size of the Me (**1**), OMe (**2**) and OEt (**3**) groups leads to the decrease in this order of the [*syn*]/[*anti*] ratio in both solvents.

Solid-state NMR

Solid-state NMR spectroscopy is the technique that provides a link between NMR data in the solution or liquid phase and results obtained from the single-crystal X-ray or neutron diffraction studies. Comparison of the isotropic chemical shifts and further structural results that characterise the geometry of molecules in the crystal lattice offers the possibility for drawing conclusions regarding changes of conformation and configuration, as well as the nature of the intermolecular contacts.

Although under fast sample rotation (8400–12 000 Hz) the spinning sidebands in CP/MAS spectra coming from aromatic carbons can be removed from the interesting region of chemical shifts, there remain problems with the interpretation of the spectra. The lower line resolution (compared to the liquid phase) leads to overlap, which makes assignments equivocal. This problem can be partially solved by performing dipolar dephasing (DD) experiments,[16–18] which allow for removal of lines corresponding to non-quaternary carbons from the ^{13}C spectra. With a dipolar dephasing time of 40 μs, the removal efficiency is very high for CH_2, lower for CH and very low for CH_3 groups. The conventional CP/MAS spectra and dipolar dephasing spectra of samples **1**–**4** are shown in Figs. 4 and 5.

Comparing the solution chemical shifts with the isotropic values in solid state and using the information about quaternary carbons from dipolar dephasing spectra, most resonance lines of the solid-state spectra can be assigned. Only the CH lines of rings *b* and *c* and some lines of ring *a* cannot be resolved.

The simplest spectrum is shown by compound **4**. In the 142–143 ppm region, two clear lines testify to the high symmetry of the molecule. Atoms C1 and C6 in ring *c* and C8 and C13 in ring *b* are chemically equivalent. This case is possible only if the dihedral angle between rings *a* and *d* is very close to 0 or 90°. The latter orientation would lead to a distinct chemical non-equivalence of atoms C20 and C24, but that is not the case. Therefore, in the solid state ring *a* is probably coplanar to the ethanocarboximide ring *d*. It may be concluded that in solutions such a conformation also plays a role.

Compound **3** crystallises with one molecule in the asymmetric unit having an *anti* conformation of the 2′-ethoxyphenyl group. Among the compounds under investigation, sample **3** shows the best resolution of the resonance lines with clear-cut lines in the aromatic and aliphatic regions. Each C atom of the substituted phenyl ring *a* gives one line and the corresponding atoms C1/C6, C2/C5, *etc.*, are chemically non-equivalent in the solid state because ring *a* is not perpendicular to the other rings, although the deviation is only *ca.* 3° (see last column in Table 2). This non-equivalence appears distinctly in the lines for C1/C6 and C8/C13, leading to one line from C1 or C6 on the left, one line from C8 or C13 on the right and an intense line from the other two atoms in the middle. An accurate assignment of the lines to atoms C2–C5, C9–C12 and C24 is not possible in the 123–131 ppm region.

Compound **2** crystallises with two independent molecules in the asymmetric part of the unit cell. For this sample two lines of the methoxy group were found to be diagnostic and their chemical shifts differ by 3 ppm. But these two lines, A and B, have different peak areas (different intensities and line widths) although the crystal contains the two independent molecules in a 1:1 ratio. Further convincing proof, which confirms the presence of two molecules in the unit cell, is the distinction of the C21 lines, also with different peak areas A and B. It is worthy to note that in contrast to other aromatic lines, the peaks of the C20 carbon are isochronous. The group of lines at 140–142 ppm shows a line splitting in comparison to compound **3** arising from the presence of two different molecules. Since molecule 1 has a dihedral angle between rings *a* and *b* of 89°, which is very close to perpendicular, this molecule must show only a small splitting while molecule 2 leads to a distinct splitting. Therefore, the flank lines of this group may be assigned to molecule 2.

To understand why the cross-polarisation (CP) spectra show for the two independent molecules 1 and 2 in compound **2** different peak areas A and B, we have studied the CP kinetics of

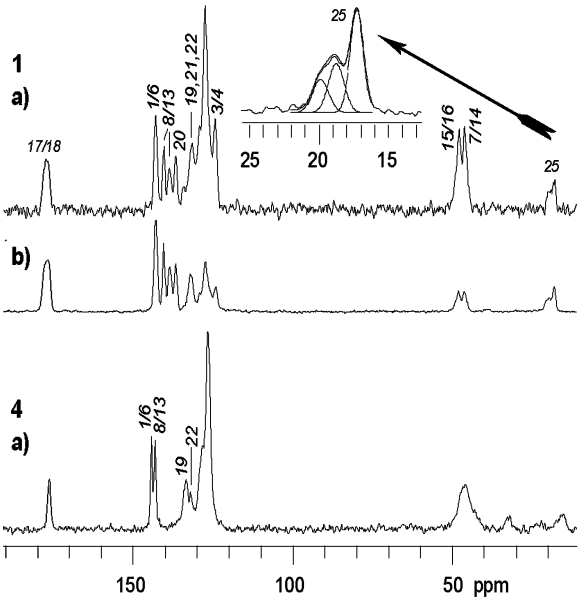

Fig. 4 ^{13}C CP/MAS spectra of **1** and **4**. (a) Conventional CP/MAS spectra; (b) CP/MAS spectrum with dipolar dephasing delay (40 μs).

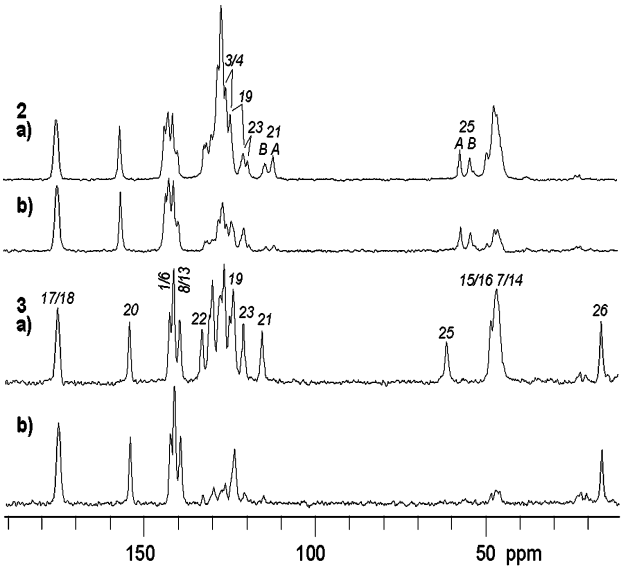

Fig. 5 ^{13}C CP/MAS spectra of **2** and **3**. (a) Conventional CP/MAS spectra; (b) CP/MAS spectra with dipolar dephasing delay (40 μs).

the C25 and C21 lines. Two models were suggested for interpretation of cross-polarisation kinetics: the I–S model and the I–I*–S model.[23] Our cross-polarisation profiles can be fitted only by the second model. This model leads to:

$$M(t) = M_0 \cdot \exp(-t/T_{1\rho H})\{1 - \lambda \cdot \exp(-t/T_{df}) - (1-\lambda)\cdot\exp[-(3t/2T_{df}) - \tfrac{1}{2}(t/T_2)^2]\}$$

In the I–I*–S model two time constants characterise the increase of polarisation transfer: T_2, which depends on the inverse direct C–H dipole-dipole interaction and leads to a steep rise of ^{13}C polarisation at starting contact times, and T_{df}, the spin diffusion from the neighbouring protons to the direct bonded ones. with a slow rise at medium contact times. A third time constant characterises the decrease of magnetisation: $T_{1\rho H}$ is the relaxation time of protons in the rotating frame. The fourth parameter depends theoretically on the number n of directly bonded protons: $\lambda = 1/(n+1)$ but in practice λ and the other CP kinetic parameters depend on group mobility. A higher mobility would imply a lower efficiency of cross-polarisation (longer T_2 and T_{df})[23,24] and a higher proton relaxation rate, $1/T_{1\rho H}$. Since an accurate determination of T_2 is difficult we focus our attention on T_{df}.

Figs. 6 and 7 show that the reason for the different intensities is the different efficiency of cross-polarisation for both molecules. The strength of the dipole-dipole C–H interaction cannot be the cause of the different kinetics of peaks A and B because the direct C–H bond lengths are equal for C25 in both molecules and also for C21. The reason for this effect must be the different mobility. Therefore, we conclude that the more intense peaks A with a higher cross-polarisation efficiency arise from the more rigid molecule 2. This molecule shows lower thermal factors and has, furthermore, many intermolecular CH/π contacts in the crystal lattice, in contrast to molecule 1 (see the section on crystal studies).

In the case of sample **1**, the methyl group peak has the highest diagnostic value. In the crystal lattice, one *syn* and two *anti* conformations exist and the presence of a broad peak for the methyl signal indicates several overlapping lines, corresponding with different conformations. From deconvolution of the signal (see top inset in Fig. 4) it is apparent that the signal can be decomposed into three components with the following characteristics: (i) 19.8 ppm, 92 Hz, 23%; (ii) 18.7 ppm, 81 Hz, 26%; (iii) 17.2 ppm, 73 Hz, 51% (chemical shift, line width, content, respectively). According to the liquid NMR

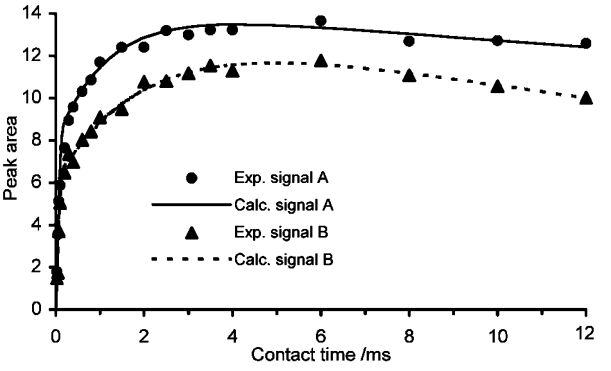

Fig. 6 Dependence of the efficiency of cross-polarisation *versus* contact time for the CH_3 group (C25) lines in **2**. The experimental points were fitted with the equation for a I–I*–S kinetic model. For details see ref. 23. Line A: $M_0 = 14.4$, $T_2 = 0.06$ ms, $T_{df} = 1.2$ ms, $T_{1\rho H} = 81$ ms, $\lambda = 0.45$; line B: $M_0 = 14.6$, $T_2 = 0.06$ ms, $T_{df} = 2.3$ ms, $T_{1\rho H} = 32$ ms, $\lambda = 0.58$.

assignment the low-field components belong to the *anti* conformations and the high-field one to the *syn* conformation.

Conclusions

A detailed knowledge of the nature of CH/π interactions on the ground of experimental and theoretical chemistry is still a challenge for organic chemists.[25] Hence models, which shed light on this problem, as well as analytical methods, which allow to search for CH/π forces, are strongly needed. In this work we revealed the power of a multi-technique approach to the structural studies of organic solids and an understanding of the importance of weak intermolecular contacts in *N*-(2′-substituted phenyl)-9,10-dihydro-9,10-ethanoanthracene-11, 12-dicarboximides. Each technique provides evidence confirming the presence of CH/π intra- and/or intermolecular interactions in the system under investigation. From X-ray diffraction it is clear that a small change in molecular design causes significant changes in crystal structure. Each *N*-(2′-substituted) compound crystallises in a different molecular system and space group. This studies provide convincing proof that the conformation in the crystal lattice is determined by CH/π forces. For sample **1** with small (2′-methyl) substituents where there are no such contacts the *syn* and *anti* conformers can coexist. For larger substituents (2′-methoxy, ethoxy group) aliphatic residues can find another molecule in the lattice that fulfills geometrical requirements and contributes to CH/π intermolecular contacts. In such case only *anti* conformers are formed. The differences in molecular packing are easily recognised by solid-state NMR. Additionally, this technique

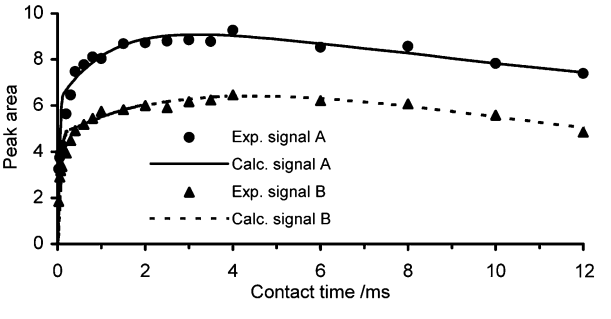

Fig. 7 Dependence of the efficiency of cross-polarisation *versus* contact time for the CH group (C21) lines in **2**. The experimental points were fitted with the equation for a I–I*–S kinetic model. For details see ref. 23. Line A: $M_0 = 10.2$, $T_2 = 0.04$ ms, $T_{df} = 1.25$ ms, $T_{1\rho H} = 38$ ms, $\lambda = 0.4$; line B: $M_0 = 10.4$, $T_2 = 0.06$ ms, $T_{df} = 4.5$ ms, $T_{1\rho H} = 17.5$ ms, $\lambda = 0.55$.

provides complementary information about molecular dynamics in the crystal lattice although not always in a direct way. The example of compound **2** with two independent molecules in the unit cell is convincing. The more rigid molecule 2, with restricted motion due to several CH/π interactions and the proximity of a large number of protons in the local environments, reveals a higher cross-polarisation efficiency. Finally, application of high-field liquid state NMR spectroscopy allowed us to assign all ^{1}H and ^{13}C signals and to revise the incorrect assignment of some ^{13}C signals in the older literature.[6e] The solute-solvent interactions influence the *syn*/*anti* ratio of conformers in the liquid phase. In the case of chloroform the solvent, which participates in CH/π contacts on the upside face of ring *b*, restricts the possibility of intramolecular interactions between the aliphatic residue and aromatic ring *b* in the *syn* conformation and as a consequence, the amount of *anti* conformer increases.

Acknowledgements

This work was supported by the Polish Committee for Scientific Research, KBN, grant no. 3 T09A 02619. GG acknowledges the European Community for financial support of his one month stay in Lodz under the Centers of Excellence program.

References

1 G. R. Desiraju and T. Steiner, *The Weak Hydrogen Bond in Structural Chemistry and Biology*, Oxford University Press/International Union of Crystallography, Oxford, 2001.
2 J. M. Lehn, *Supramolecular Chemistry, Concepts and Perspectives*, VCH Weinheim, New York, Basel, Cambridge, Tokyo, 1995; G. R. Desiraju, *Acc. Chem. Res.*, 2002, **35**, 565.
3 G. R. Desiraju, *Angew. Chem., Int. Ed. Engl.*, 1995, **34**, 2311.
4 (*a*) D. J. Evans, P. C. Junk and M. K. Smith, *New J. Chem.*, 2002, **26**, 1043; (*b*) N. Motohiro and H. Minoru, *Tetrahedron*, 1989, **45**, 7201
5 K. Kishikawa, K. Yoshizaki, S. Kohmoto, M. Yamamoto, K. Yamaguchi and K. Yamada, *J. Chem. Soc., Perkin Trans. 1*, 1997, 1233.
6 (*a*) S. M. Verma and N. B. Singh, *Aust. J. Chem.*, 1976, **29**, 295; (*b*) V. Singh and R. M. Singh, *Indian J. Chem. B*, 1984, **8**, 782; (*c*) K. K. Srivastav, A. K. Verma and S. M. Verma, *Indian J. Chem., Sect. B: Org. Chem. Incl. Med. Chem.*, 1993, **32**, 1143; (*d*) A. Srivastava, V. Srivastava and S. M. Verma, *Indian J. Chem., Sect. B: Org. Chem. Incl. Med. Chem.*, 1998, **37**, 1030; (*e*) N. Srivastava, V. Srivastava and S. M. Verma, *Indian J. Chem., Sect. B: Org. Chem. Incl. Med. Chem.*, 1991, **30**, 1080
7 (*a*) M. J. Potrzebowski, M. Michalska, A. E. Kozioł, S. Kaźmierski, T. Lis, J. Pluskowski and W. Ciesielski, *J. Org. Chem.*, 1998, **63**, 4209; (*b*) M. J. Potrzebowski, G. Grossmann, K. Ganicz, S. Olejniczak, W. Ciesielski, A. E. Kozioł, I. Wawrzycka, G. Bujacz, U. Haeberlen and H. Schmitt, *Chem.–Eur. J.*, 2002, **8**, 2691.
8 The used numeration is convenient for crystal structure and NMR, but does not conform with the numeration in the names of the compounds.
9 E. Weber, S. Finge and I. Csöregh, *J. Org. Chem.*, 1991, **56**, 7281.
10 B. A. Frenz, SDP–Structure Determination Package, Enraf–Nonius, Delft, 1984.
11 A. C. T. North, D. C. Philips and F. S. Mathews, *Acta Crystallogr., Sect. A*, 1968, **24**, 351.
12 G. M. Sheldrick, G. M. Kruger and R. Goddard, SHELXS-86, Crystallographic Computing 5, Oxford University Press, Oxford, 1990.
13 G. M. Sheldrick, SHELXL-93, Program for Crystal Structure Refinement, University of Göttingen, Germany,1993.
14 G. Metz, X. Wu and S. O. Smith, *J. Magn. Reson.*, 1994, **110**, 219.
15 A. E. Bennet, C. Rienstra, M. Auger, C. Lakami and R. Griffin, *J. Chem. Phys.*, 1995, **103**, 6951.
16 M. Alla and E. Lippmaa, *Chem. Phys. Lett.*, 1976, **37**, 260.
17 S. J. Opella and M. H. Frey, *J. Am. Chem. Soc.*, 1979, **101**, 5854.
18 J. Witt, D. Fenzke and W. D. Hoffmann, *Appl. Magn. Reson.*, 1992, **3**, 151.
19 WIN-NMR 6.0 Program, Version 960901, Bruker–Franzen Analytik GmbH, Bremen, 1996.
20 M. Nishio, M. Hirota and Y. Umezawa, in *Methods in Stereochemical Analysis*, ed. A. P. Marchand, Wiley–VCH, New York, 1998, p. 19 and p. 33.
21 The 12 protons of the dihydroethanoanthracene skeleton appear in the spectra as three particular spin systems for each conformation. The aliphatic protons H7/14 and H15/16 on the one hand and the ring *c* protons H2/5 and H3/4 on the other hand give approximately AA′XX′ spin systems, while the signals from the ring *b* protons H9/12 and H10/11 must be interpreted as AA′BB′ spin systems. The coupling constants (Hz) of the aliphatic system in all investigated compounds differ only slightly: ^{3}J(14–15) = 8.4(2), ^{4}J(7–15) = −0.2(1), ^{3}J(15–16) = 8.0(2), and ^{5}J(7–14) = 0.0(1). The coupling constants in both aromatic spin systems were: ^{3}J(2–3 and 9–10) = 7.3(1), ^{4}J(2–4 and 9–11) = 1.3(1), ^{3}J(3–4 and 10–11) = 7.6(1), and ^{4}J(3–5 and 10–12) = 0.6(1).
22 The authors of ref. 6e have made an attempt to assign some ^{13}C lines to the atoms of compounds **1**, **2**, **4** and others. Our 2D spectra show that some of the assumed assignments are not correct.
23 W. Kolodziejski and J. Klinowski, *Chem. Rev.*, 2002, **102**, 613 and references cited therein.
24 R. Voelkel, *Angew. Chem., Int. Ed. Engl.*, 1988, **27**, 1468.
25 J. Ribas, E. Cubero, F. J. Luque and M. Orozco, *J. Org. Chem.*, 2002, **67**, 5976 and references cited therein.